J. of Supercritical Fluids 54 (2010) 81–88

Contents lists available at ScienceDirect

The Journal of Supercritical Fluids

journal homepage: www.elsevier.com/locate/supflu

Investigation of the degree of homogeneity and hydrogen bonding in PEG/PVP blends prepared in supercritical CO_2: Comparison with ethanol-cast blends and physical mixtures

Philip W. Labuschagne [b,*], Maya J. John [a], Rotimi E. Sadiku [b]

[a] CSIR, Materials Science and Manufacturing, Port Elizabeth 6000, South Africa
[b] Tshwane University of Technology, Department of Polymer Technology, Private Bag X 025, Lynnwoodridge 0040, South Africa

ARTICLE INFO

Article history:
Received 4 February 2010
Received in revised form 15 March 2010
Accepted 27 March 2010

Keywords:
Supercritical fluids
Polymer blends
H-bonding
Diffusion

ABSTRACT

The degree of homogeneity and H-bond interaction in blends of low-molecular-mass poly(ethylene glycols) (PEG, M_w = 400, 600, 1000) and poly(vinylpyrrolidone) (PVP, $M_w = 9 \times 10^3$) prepared in supercritical CO_2, ethanol and as physical mixtures were studied by differential scanning calorimetry (DSC), Fourier-transform infrared (FTIR) spectroscopy and dynamic mechanical analysis (DMA) techniques. Homogeneity of samples prepared in supercritical CO_2 were greater than physically mixed samples, but slightly less than ethanol-cast samples. PEG–PVP H-bond interaction was higher for ethanol-cast blends when compared to blends prepared in supercritical CO_2. This reduced interaction was attributed to a combination of: (1) shielding of PEG–PVP H-bond interactions when CO_2 is dissolved in the blend; (2) rapidly reduced PEG and PVP chain mobility upon CO_2 venting, delaying rearrangement for optimum PEG–PVP H-bond interaction.

1. Introduction

CO_2 is known to interact, via Lewis acid–base interactions, with polymers containing electron-donating oxygen or fluorine atoms present in the functional groups or backbone [1]. Such interactions lead to swelling and subsequent plasticisation of polymers. This has allowed supercritical CO_2 to be used as medium for various polymer processes such as: particle formation, blending, impregnation, foaming, chemical modifications, etc. [2–5].

One application for which supercritical CO_2 has received considerable attention is as a processing medium in the preparation of drug–polymer delivery systems [6–9]. This stems mainly from supercritical CO_2's ability to provide non-toxic and low temperature processing conditions when compared to conventional preparation methods in which toxic solvents or high temperatures are required for processing. So far, supercritical CO_2 has been successfully used in the encapsulation, micronization, coating and impregnation of many drugs [10–17].

In most drug delivery systems, the drug is dispersed or encapsulated within a single biodegradable or bioerodible polymer [9]. The role of the polymer is to protect the drug from degradation and to ensure controlled delivery to the targeted site. Drug release occurs either via diffusion through the polymer matrix or due to erosion of the polymer itself [18]. Alternative drug delivery systems are produced when two polymers form a strong association through interaction between complementary functional groups. The result of such interpolymer association (usually through H-bonding) is called interpolymer complexation and produces a drug delivery system in which the properties of the interpolymer complex is completely different from the constituent polymers [19]. One such example is the interpolymer complexation between polyvinylpyrrolidone (PVP) and poly(ethylene glycol) (PEG) [20]. H-bonding occurs between the terminal hydroxyl groups of short chain PEG molecules (M_w: 200–600) and the carbonyl groups of long chain PVP molecules (M_w: 1×10^6), resulting in a high free-volume structure of PVP chains crosslinked by flexible PEG chains. Hydration of this complex to equilibrium moisture content forms a hydrogel which yields a product with high elasticity and excellent adhesive strength. Combined with controlled release characteristics, such PVP–PEG hydrogels can be employed as drug-loaded adhesive patches in transdermal delivery devices [21].

Of specific interest is that both PEG and PVP can be plasticised in supercritical CO_2 due to the presence of electron-donating ether and carbonyl groups in PEG and PVP molecules, respectively. Many authors have studied various aspects of PEG-CO_2 systems [22–27] while PVP is often the polymer of choice for increasing the bioavailability of hydrophobic drugs through supercritical CO_2 assisted impregnation into PVP [10,28,29].

In addition, H-bond interactions have been shown to occur in the presence of CO_2 as demonstrated with dye and drug impregna-

* Corresponding author. Tel.: +27 12 841 2149; fax: +27 12 841 3553.
E-mail address: plabusch@csir.co.za (P.W. Labuschagne).

0896-8446/$ – see front matter © 2010 Elsevier B.V. All rights reserved.
doi:10.1016/j.supflu.2010.03.012

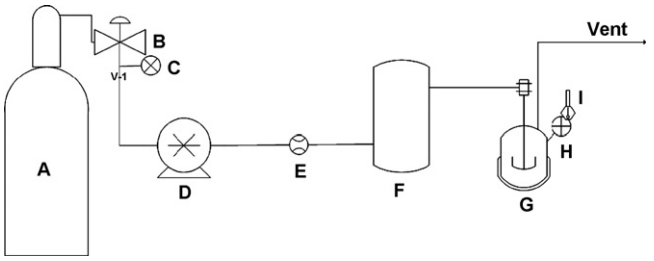

Fig. 1. Schematic diagram of the supercritical CO_2 reactor: (A) CO_2 cylinder, (B) back-pressure regulator, (C) pressure gauge, (D) diaphragm pump, (E) flow meter, (F) CO_2 pre-heater, (G) mixing chamber, (H) pressure gauge, (I) temperature probe.

tions into polymers [3,10]. Ngo et al. [3] studied various conditions under which azo-dyes would impregnate into PMMA using supercritical CO_2 as processing medium. The degree of impregnation was determined by the partition coefficient (K_c) of the system, i.e. the ratio of dye concentration in polymer to dye concentration in supercritical CO_2. Usually, the K_c for dyes is high due to high solubility of the dye in the polymer. Interestingly, it was found that K_c decreases, which was attributed to H-bonds between the dyes and the PMMA. Such H-bond interactions are believed to cause stearic hindrances, preventing other dye molecules from migrating into the polymer. Kazarian and Martirosyan [10] conducted *in situ* FTIR spectroscopic monitoring during ibuprofen impregnation into PVP. Results showed the appearance of a new carbonyl band at a lower wavenumber which they attributed to ibuprofen-PVP H-bonding.

In this chapter, an initial study was performed by comparing the level of homogeneity and H-bonding in PEG/PVP blends prepared as physical mixtures, cast from ethanol solution and in supercritical CO_2. Differential scanning calorimetry (DSC) was performed to monitor crystallinity changes, Fourier-transform infrared (FTIR) spectroscopy was used to compare wavenumber shifts associated with H-bond interactions and dynamic mechanical analysis (DMA) was used to investigate thermal transitions.

2. Experimental

2.1. Materials and methods

PEG (400 and 1000 M_w) and PEG (600 M_w) were purchased from Unilab and Fluka respectively. PVP (9000 M_w; Kollidon 17PF) was purchased from BASF. Carbon dioxide (99.995% purity) was purchased from Air Products. All PEG and PVP samples were dried for 12 h at 70 °C in a vacuum oven (Model VO65, Vismara) prior to processing. However, due to the extreme hygroscopic nature of PVP, some water was expected to be present during processing and sample analysis.

The supercritical CO_2 processing was carried out in a Separex pilot-scale reactor (Separex Equipements, Champigneulles, France), illustrated in Fig. 1. CO_2 gas was drawn from a standard commercial gas cylinder fitted with a dip-tube. CO_2 was pumped through a pre-heated chamber, set to the reactor temperature, into the mixing chamber. The mixing chamber (0.5 L capacity), was fitted with a magnetically driven stirrer and was pre-heated with electrical heaters.

ATR-FTIR spectra of the samples were obtained using a PerkinElmer Spectrum 100 FTIR spectrometer, with wavenumbers ranging from 4000 to 650 cm^{-1}. FTIR analysis confirmed the complete release of CO_2 from the sample by absence of the CO_2 absorbance band at 2334 cm^{-1}. A PerkinElmer DSC-7, calibrated with indium, was used to study the melting endotherms of the samples. Samples of 3 to 5 mg in weight were sealed in aluminium pans with pierced lids and scanned at a heating rate of 20 °C/min from −20 to 70 °C. DMA was performed with a PerkinElmer DMA

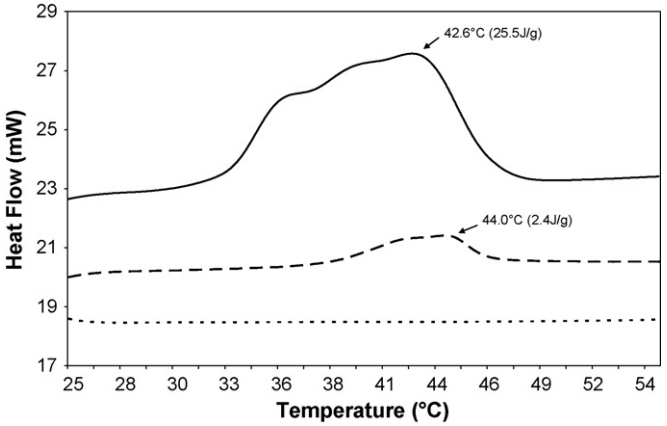

Fig. 2. DSC thermograms of the various PEG-1000-PVP mixtures: physical mixture (—); $scCO_2$-processed (– – –) and ethanol-cast (- - -).

8000. All samples (12.5 × 5 × 1 mm) were exposed to a reference frequency of 1 Hz, using a single cantilever bending deformation mode. The heating rate was 5 °C/min.

2.2. Preparation of blends

Blends of PEG/PVP were prepared by physical mixing ($blend_{phys}$), ethanol-casting ($blend_{eth}$) and supercritical CO_2 ($blend_{CO_2}$) processing. A ratio of 15/85 wt% of PEG to PVP was chosen for all experiments. $Blend_{phys}$ was prepared by mixing the ingredients in a Kenwood coffee grinder (Model:CG100) for 30 s. $Blend_{eth}$ was prepared by first adding rectified ethanol to the weighed-off ingredients in order to obtain a 20 wt% solution. The solutions were then stirred with a spatula until all the material was dissolved. The solutions were placed in an oven, set at 60 °C for 48 h, after which it was placed in a vacuum oven (Model VO65, Vismara), set at 60 °C until all ethanol was removed (as monitored by an absence of ethanol FTIR absorbance band at 1045 cm^{-1}). The remaining material was then ground to a powder in a coffee grinder. $Blend_{CO_2}$ was prepared by first mixing the weighed-off ingredients (20 g samples) in the coffee grinder for 30 s, and then placed in the supercritical CO_2 reactor, pre-heated to 40 °C. The reactor was sealed and charged with CO_2 up to a pressure of 200 bar. After allowing for 1 h for reaching equilibrium, the mixture was stirred intermittently over a 2-h period at 100 rpm. Following processing, the CO_2 pump was switched off and all the CO_2 in the reactor was released over a period of ca. 3 min. The material was removed from the reactor, and then ground to a powder in a coffee grinder. All the blends were stored in airtight containers in a humidity and temperature controlled laboratory, prior to analysis.

3. Results and discussion

3.1. Differential scanning calorimetry

DSC thermograms of the PVP blends with PEG-1000 are presented in Fig. 2. The weight fraction of crystalline PEG-1000 after blending with PVP (w_{crPEG}) was calculated as follows:

$$w_{crPEG} = \frac{\Delta H_{blend}}{w_{PEG} \cdot \Delta H_{PEG}} \quad (1)$$

where ΔH_{blend} is the heat of fusion of the PEG-1000–PVP blend, w_{PEG} the weight fraction of PEG in the blend and ΔH_{PEG} the heat of fusion of the pure PEG-1000. Based on this calculation, w_{crPEG} is 1.1 for $blend_{phys}$, 0.1 for $blend_{CO_2}$ and 0 for $blend_{eth}$. It is likely that the large reductions in crystalline PEG-1000 in $blend_{eth}$ and $blend_{CO_2}$ are due to PEG mobility restrictions imposed either by H-bond

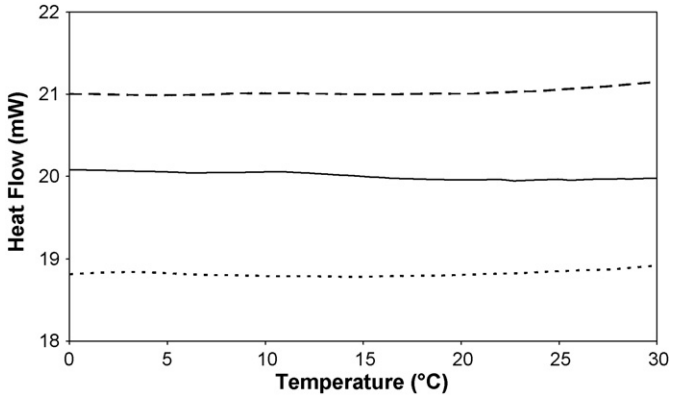

Fig. 3. DSC thermograms of the various PEG-600/PVP mixtures: physical mixture (—); $scCO_2$-processed (– – –) and ethanol-cast (- - -).

interactions between PEG and PVP molecules or by entrapment in a rigid PVP matrix, or both. This indicates a high level of inter-dispersion. The high degree of crystalline PEG-1000 in $blend_{phys}$ indicates poor inter-dispersion. This can be expected since the samples were prepared at room temperature, which is below the melting range of PEG-1000 (Onset: 33 °C; T_m: 45.6 °C).

Neither of the processing methods containing PEG-600 (Fig. 3) or PEG-400 (Fig. 4) exhibits any crystalline PEG melting peak. Most likely, the increased mass transport properties induced by supercritical CO_2 and ethanol media assisted in the homogenous mixing of PEG and PVP molecules [3,30,31]. Upon removal of CO_2 and the ethanol, the well-dispersed PEG molecules easily interact with the PVP molecules, preventing recrystallisation. The absence of a crystalline PEG melting peak in $blend_{phys}$ can be attributed to rapid self-diffusion of the PEG molecules, followed by immobilisation due to H-bond interaction with PVP molecules [32]. The low w_{PEG} would also suggest that, after self-diffusion, all PEG molecules become immobilised in this way [33].

3.2. Dynamic mechanical analysis

Analysis of the dynamic mechanical properties of these polymer blends over a wide temperature range would give insight into the visco-elastic properties of the materials. Variations in storage modulus (E'), an indication of rigidity, and damping factor (Tan δ), which is the ratio of energy dissipated as heat to the maximum energy stored in the sample and which indicates the balance of viscous to elastic behaviour were studied. The Tan δ peak temperature is also related to the glass transition temperature (T_g) of the material. However, T_g derived from DMA can be between 10–30 °C higher than that derived from DSC, depending on conditions such as frequency and heating rates, respectively [34–36].

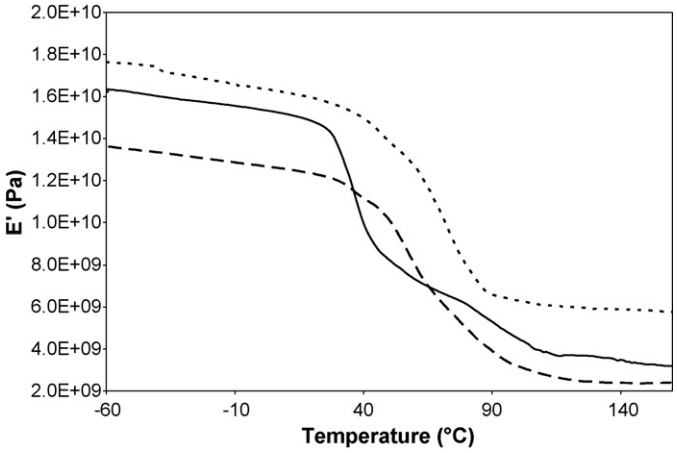

Fig. 5. E' curves of the PEG-1000–PVP mixtures: physical mixture (—); $scCO_2$-processed (– – –) and ethanol-cast (- - -).

In the samples containing PEG-1000, $blend_{eth}$ show the highest E' and $blend_{CO_2}$ the lowest (Fig. 5). This could be attributed to some degree of H-bonding between PEG-1000 and PVP in $blend_{eth}$, thereby enhancing the cohesive strength of the material. While PEG-1000 blends with PVP are generally regarded as immiscible due to low PEG hydroxyl content, miscibility studies have not yet been conducted at such low PEG-1000 concentrations [37]. Perhaps greater intimate mixing and lower amounts of PEG ether groups competing with PVP carbonyl group for H-bond interaction are contributing factors.

The Tan δ curve of $blend_{phys}$, and to a lesser extent $blend_{CO_2}$, show multimodal behaviour (Fig. 6), while the sharpness of the Tan δ curve for $blend_{eth}$ (Fig. 6) confirms greater homogeneity. In $blend_{phys}$, there is a minor peak at 37 °C, a prominent peak at 106 °C and a shoulder peak at 130 °C. These peak temperatures are possibly the result of PEG-rich and PEG-poor domains. The Tan δ curve of $blend_{CO_2}$ largely exhibits morphological homogeneity similar to $blend_{eth}$, however the shoulder at ca.106 °C shows some evidence of heterogeneity. Tan δ generally decreases when there is less freedom of movement of the polymer chains, ether through reinforcement [38], crystallisation [39] or closer packing, i.e. stereo-

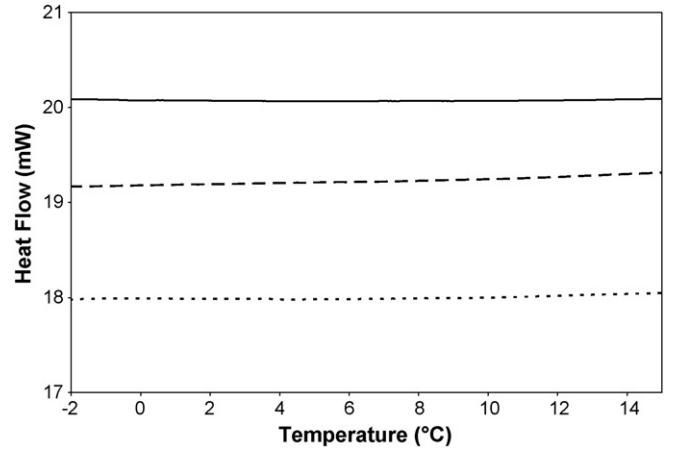

Fig. 4. DSC thermograms of the various PEG-400/PVP mixtures: physical mixture (—); $scCO_2$-processed (– – –) and ethanol-cast (- - -).

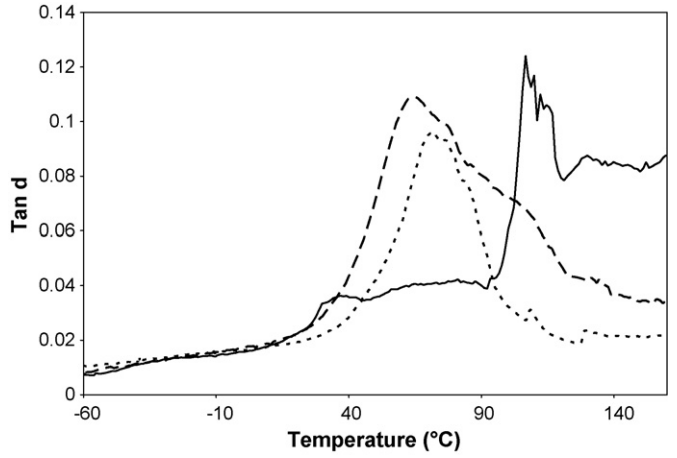

Fig. 6. Tan δ curves of the PEG-1000–PVP mixtures: physical mixture (—); $scCO_2$-processed (– – –) and ethanol-cast (- - -).

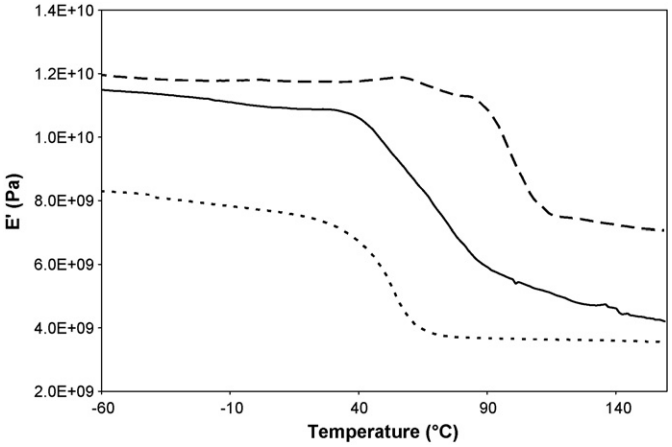

Fig. 7. E' curves of the PEG-600–PVP mixtures: physical mixture (—); $scCO_2$-processed (– – –) and ethanol-cast (- - -).

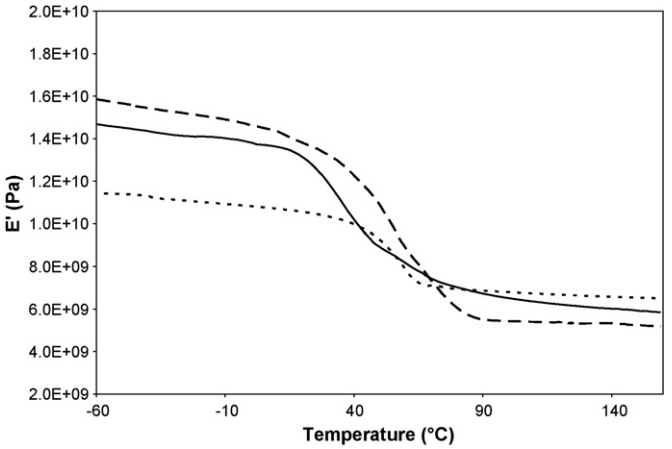

Fig. 9. E' curves of the PEG-400–PVP mixtures: physical mixture (—); $scCO_2$-processed (– – –) and ethanol-cast (- - -).

complexation [40]. Tan δ values are lowest for $blend_{eth}$ indicating restricted molecular mobility, which could be ascribed to greater H-bonding within the PEG–PVP blend.

DMA thermograms of the samples with PEG-600 (Figs. 7 and 8) show a reduction in E' and Tan δ for all processing methods. Such an overall decrease is characteristic of greater elastic-like behaviour [41]. The overall increase in plasticisation is probably due to inter-polymer complexation between PEG-600 and PVP in which both terminal hydroxyls of PEG-600 form a H-bond with PVP. This results in a carcass-like structure of great free volume [20]. The most significant reduction in E' is found with $blend_{eth}$. $Blend_{phys}$ relies on self-diffusion of the PEG-600 molecules for intimate mixing, however immobilisation due to H-bonding with PVP molecules limit the movement of PEG-600 molecules [32]. $Blend_{CO_2}$ displays similar plasticisation than $blend_{phys}$, although a much higher T_g than both $blend_{phys}$ or $blend_{eth}$.

$Blend_{eth}$ and $blend_{CO_2}$ display similar Tan δ peak heights, indicating slightly more elastic behaviours than $blend_{phys}$. However, as indicated, T_gs varies significantly (52.2 and 95.6 °C, respectively). $Blend_{eth}$ also shows a narrow peak, suggesting greater morphological uniformity. $Blend_{phys}$ shows slightly less elastic behaviour as indicated by the higher Tan δ values. In addition, a very broad peak is shown, indicating less uniform morphology.

An interesting observation with samples containing PEG-400 is that E' is higher in all samples compared to those with PEG-600 (Fig. 9). This is an indication of greater reinforcement, possibly due to PEG–PVP H-bonding. However, it is only $blend_{eth}$ which also show an increase in T_g, while $blend_{phys}$ and $blend_{CO_2}$ show a slight decrease in T_g.

The Tan δ peak of $blend_{phys}$ (Fig. 10) is broader when compared to both $blend_{eth}$ and $blend_{CO_2}$, indicating a greater degree of morphological heterogeneity. The lower Tan δ value, accompanied by a higher T_g of $blend_{eth}$ would suggest a close-knit structure of PVP and PEG-400 molecules, where the PEG-400 molecules are thought to be evenly dispersed in between the PVP molecules and H-bonded. The height and width of the Tan δ peak of $blend_{CO_2}$ indicate some degree of homogeneity and a level of PEG–PVP interaction that is deemed intermediate between that of $blend_{eth}$ and $blend_{phys}$. This would suggest improved PEG–PVP inter-dispersion, but not reaching the same level of H-bond interaction found in $blend_{eth}$.

3.3. Infrared spectroscopy

Infrared spectroscopy is one of the most powerful tools to detect H-bonding between polymers. The degree of H-bonding interactions can be inferred from changes in the peak position of the C=O stretching band where H-bonding is evidenced by a shift to lower wavenumbers [20].

Fig. 11 (left) displays the ATR spectra of the various PEG–PVP blends in the region 1760–1560 cm^{-1}. The absorption bands in this region represent the ν(C=O) stretching band of PVP in differ-

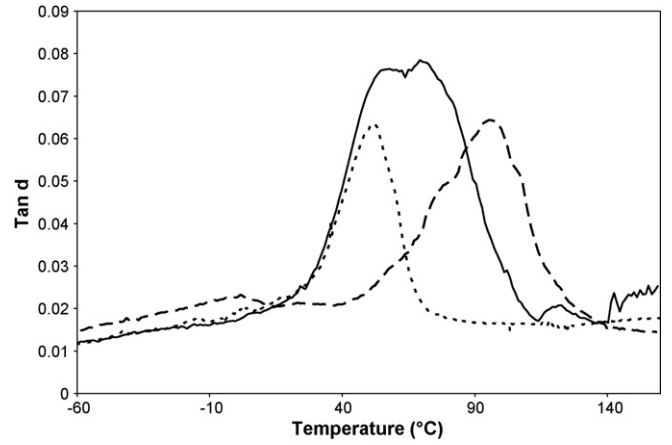

Fig. 8. Tan δ curves of the PEG-600–PVP mixtures: physical mixture (—); $scCO_2$-processed (– – –) and ethanol-cast (- - -).

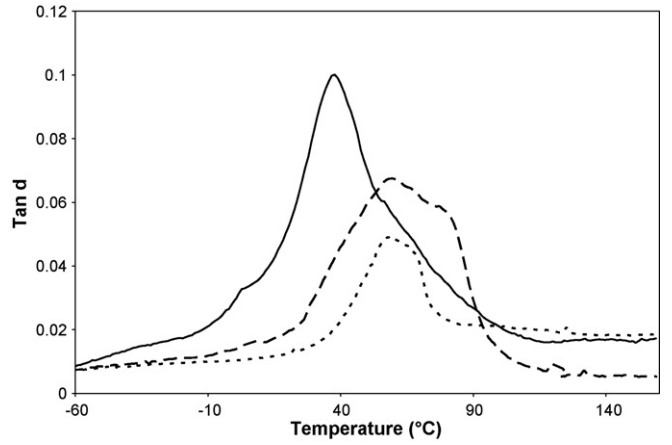

Fig. 10. Tan δ curves of the PEG-400–PVP mixtures: physical mixture (—); $scCO_2$-processed (– – –) and ethanol-cast (- - -).

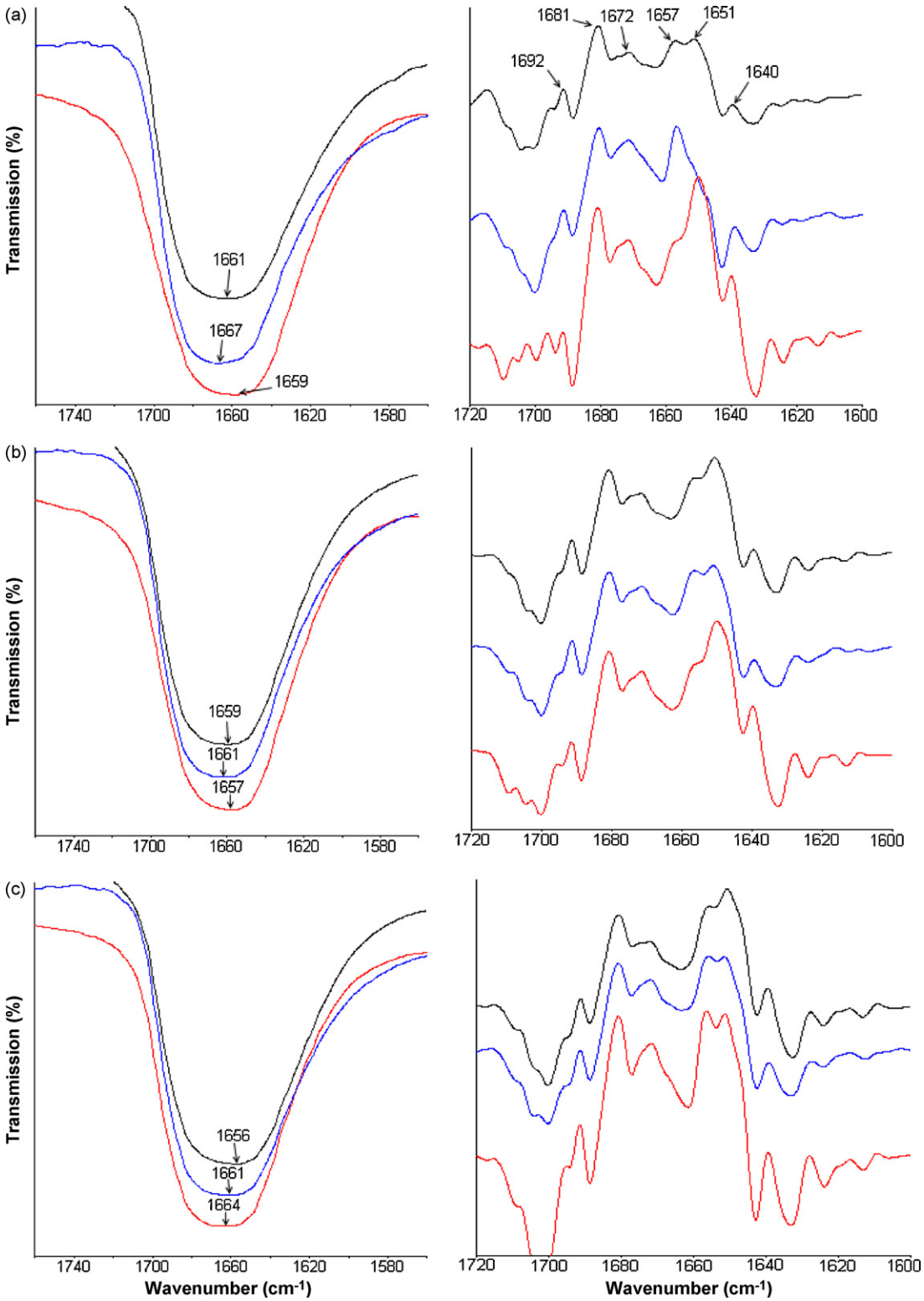

Fig. 11. Transmission IR spectra with corresponding second derivative spectra of the C=O region of PVP blends with PEG-1000 (a), PEG-600 (b) and PEG-400 (c) prepared by: physical mixing ( ); $scCO_2$-processing ( ); and solvent casting ( ). (For interpretation of the references to colour in this figure legend, the reader is referred to the web version of the article.)

ent blends. These bands show minor, but significant differences, which can be better appreciated by studying the corresponding second derivative spectra. These spectra show that the ν(C=O) band actually consists of a multitude of smaller bands. These bands can broadly be assigned as follows: carbonyl groups that are unassociated (>1680 cm^{-1}) [42,43], bound by PVP-PVP dipole interactions or weakly H-bonded to another species (ca. 1679–1665 cm^{-1}) [31,44,45] and strongly H-bonded to another species (<1664 cm^{-1}) [45–47].

The important bands in this study are those attributed to H-bonded carbonyl groups. However, due to the strong hygroscopic nature of PVP, present water molecules can complicate elucida-

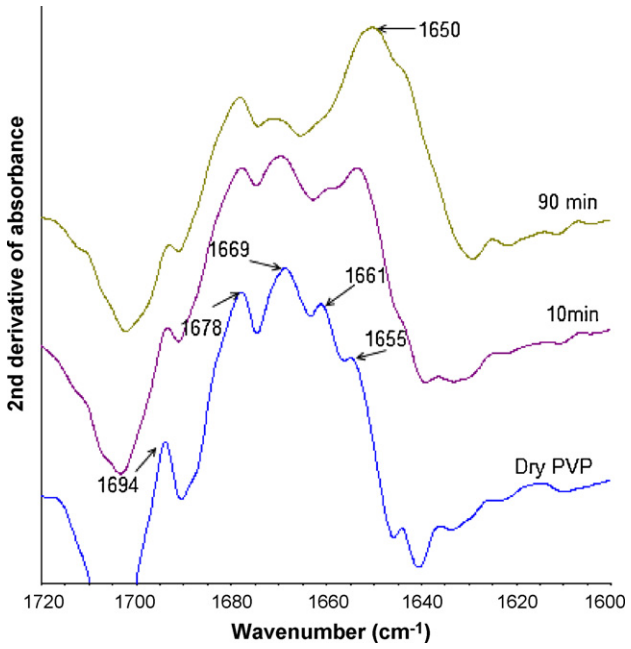

Fig. 12. 2nd derivative FTIR profiles of the carbonyl band of PVP exposed to atmospheric humidity over a period 90 min.

tion of H-bonding interactions between PEG and PVP using FTIR spectroscopy. To determine whether effects of present water can be ignored, second derivative spectra of dried and hydrated PVP are compared. Fig. 12 shows bands at 1694, 1678, 1669, 1661 and 1655 cm^{-1} in the dried PVP. Upon exposure to atmospheric moisture, the intensity of the band at 1655 cm^{-1} increases, and shifts to 1650 cm^{-1}. In the PEG–PVP blends, strong bands are seen at 1681, 1657 and 1651 cm^{-1}. Feldstein et al attributed the band at 1680 cm^{-1} to PEG which is loosely bound (through only one terminal hydroxyl group) to PVP, and bands at 1655 and 1650 cm^{-1} to strong H-bond interaction between PEG and PVP [45]. Clearly, there is some overlap in the 1655–1650 cm^{-1} region that can be attributed to either PVP–water or PVP–PEG interaction, or both. Nevertheless, the second derivate spectra of Fig. 11a (PEG-1000–PVP) in the same absorption region shows clear differences between the different preparation methods. DMA and DSC analysis also showed the greatest difference in properties with blends containing PEG-1000. In fact, for $blend_{eth}$, DSC analysis showed a complete absence of crystalline PEG-1000, while DMA analysis showed the greatest E' values which we attributed to some degree of H-bonding. Studying Fig. 11a shows the greatest intensity of the 1651 cm^{-1} band in $blend_{eth}$. This, if taken as indication of greater H-bond interaction between PEG and PVP, this would correspond with the DSC and DMA results. Thus, it would seem acceptable to use relative intensities of these bands to evaluate H-bond interaction in the different preparation methods.

The general trend in Fig. 11(a)–(c) shows that by decreasing PEG M_w, variations in H-bond interaction behaviour between the various processing methods becomes smaller. This is likely due to increased diffusion coefficients found with decreasing M_w of PEG. Consequently, the greatest variations in H-bonding are found with blends containing PEG-1000, where both $blend_{phys}$ and $blend_{CO_2}$ show evidence of reduced H-bond interaction, when compared to $blend_{eth}$. In $blend_{phys}$, this may be the result of poor PEG-1000/PVP inter-dispersion as indicated by DSC and DMA analyses. Both showed evidence of intact PEG-1000 crystallites and morphological heterogeneity. $Blend_{CO_2}$ showed evidence of greater PEG-1000 inter-dispersion, but this did not result into the same levels of H-bond interaction with PVP, as found with $blend_{eth}$.

The discrepancy concerning the level of H-bond interaction between $blend_{eth}$ cast and $blend_{CO_2}$ is attributed to a combination of factors, namely: shielding effects of CO_2 molecules and the time-dependence for PEG–PVP H-bond interaction to reach equilibrium. Due to favourable Lewis acid–base interaction between CO_2 and the electron-donating ether and carbonyl groups of PEG and PVP respectively [1], increased CO_2 pressure leads to increased sorption of CO_2 molecules into the polymers. This leads to swelling of the polymer, resulting in T_g depression of amorphous polymers (i.e. PVP) and T_m reduction of semi-crystalline polymers (i.e. PEG) [22,48]. Increased chain mobility results in enhanced diffusion coefficients [3,30,49,50] and thus polymer inter-diffusion [31]. This results in greater blend homogeneity. However, CO_2 molecules interacting with PVP carbonyl groups, effectively reduce H-bond interaction between PEG and PVP molecules [31]. Thus, while CO_2 dissolution into the blend enhances PEG–PVP inter-dispersion, H-bond interaction is not favoured. After CO_2 venting, no barriers to PEG–PVP interaction exist, but there remains a time-dependence for rearrangement of PEG molecules into an equilibrium state of H-bond interaction with PVP molecules [33,51]. Due to the prolonged drying schedule for removing all traces of ethanol in $blend_{eth}$, sufficient time was allowed for PEG chains to rearrange and form stable associates with PVP molecules. However, for $blend_{CO_2}$, CO_2 venting occurred within a couple of minutes, resulting in a rapid decrease in polymer diffusion coefficients. Thus, a significantly shorter period for PEG redistribution was available.

Poor homogeneity was observed for $blend_{phys}$, although some degree of H-bonding with PVP occurred. Dissolution of low M_w PEG molecules into the PVP matrix is mainly facilitated by their plasticising effect [52]. However, diffusion of PEG molecules into the PVP matrix may be restricted through H-bond interaction with PVP molecules [31]. With PEG-1000 being solid, no self-diffusion can occur as shown with the intact crystalline domains. However, FTIR spectroscopic analysis demonstrates the presence of some H-bond interaction between PEG-1000 and PVP. It is possible that PVP molecules adsorb onto the surface of such crystalline domains, forming H-bonds with outwardly exposed terminal hydroxyl groups [37].

4. Conclusions

The ability of PVP to form a homogenous H-bonded mixture with low M_w PEG (M_w: 400, 600 and 1000) lies in the molecules being properly dispersed, experiencing no barriers for interaction and having sufficient mobility to allow for self-diffusion into thermodynamically favourable arrangements. In $blend_{eth}$, these conditions were met, allowing homogenous mixtures of PEG/PVP with a high degree of H-bonding. With CO_2 dissolution into the PEG–PVP blends, weak Lewis acid–base interaction with the polymers results in increased chain mobility, which in turn allows the formation of homogenous PEG–PVP mixtures. However, $blend_{CO_2}$ showed lower H-bond interaction when compared to $blend_{eth}$. This was attributed to a combination of factors: (1) CO_2 molecules interacting with PVP carbonyl groups limit PEG–PVP interaction, (2) once CO_2 is removed molecular mobility is severely reduced, delaying the formation of an optimally H-bonded blend. $Blend_{phys}$ showed poor homogeneity and limited H-bonding, which was mainly due to restricted mobility of the PEG and PVP chains.

These experiments were conducted under isothermal and isobaric conditions. Many variables are thus available for further optimisation. In addition to temperature and pressure, other processing variables, such as polymer M_w and PEG/PVP ratios, are available.

These variables will be investigated in the next study. A valuable analytical technique, namely *in situ* FTIR spectroscopy, would give

an insight into the level of interaction between different components of polymer blends under various conditions, including how such interactions are affected during CO_2 venting.

Acknowledgements

Philip W. Labuschagne would like to thank Prof Sergei G. Kazarian for his advice and assistance and for the CSIR, South Africa for funding this research.

References

[1] S.G. Kazarian, M.F. Vincent, F.V. Bright, C.L. Liotta, C.A. Eckert, Specific intermolecular interaction of carbon dioxide with polymers, Journal of the American Chemical Society 118 (1996) 1729–1736.
[2] S.G. Kazarian, Polymer processing with supercritical fluids, Polymer Science: Series C 42 (2000) 78–101.
[3] T.T. Ngo, C.L. Liotta, C.A. Eckert, S.G. Kazarian, Supercritical fluid impregnation of different azo-dyes into polymer: in situ UV/Vis spectroscopic study, Journal of Supercritical Fluids 27 (2003) 215–221.
[4] S.P. Nalawade, F. Picchioni, L.P.B.M. Janssen, Supercritical carbon dioxide as a green solvent for processing polymer melts: processing aspects and applications, Progress in Polymer Science (Oxford) 31 (2006) 19–43.
[5] M.D. Elkovitch, L.J. Lee, D.L. Tomasko, Effect of supercritical carbon dioxide on morphology development during polymer blending, Polymer Engineering and Science 40 (2000) 1850–1861.
[6] O.R. Davies, A.L. Lewis, M.J. Whitaker, H. Tai, K.M. Shakesheff, S.M. Howdle, Applications of supercritical CO_2 in the fabrication of polymer systems for drug delivery and tissue engineering, Advanced Drug Delivery Reviews 60 (2008) 373–387.
[7] J. Fages, H. Lochard, J.J. Letourneau, M. Sauceau, E. Rodier, Particle generation for pharmaceutical applications using supercritical fluid technology, Powder Technology 141 (2004) 219–226.
[8] P.J. Ginty, M.J. Whitaker, K.M. Shakesheff, S.M. Howdle, Drug delivery goes supercritical, Materials Today 8 (2005) 42–48.
[9] A. Tandya, R. Mammucari, F. Dehghani, N.R. Foster, Dense gas processing of polymeric controlled release formulations, International Journal of Pharmaceutics 328 (2007) 1–11.
[10] S.G. Kazarian, G.G. Martirosyan, Spectroscopy of polymer/drug formulations processed with supercritical fluids: in situ ATR-IR and Raman study of impregnation of ibuprofen into PVP, International Journal of Pharmaceutics 232 (2002) 81–90.
[11] A. Argemí, A. Vega, P. Subra-Paternault, J. Saurina, Characterization of azacytidine/poly(L-lactic) acid particles prepared by supercritical antisolvent precipitation, Journal of Pharmaceutical and Biomedical Analysis 50 (2009) 847–852.
[12] A.R. Sampaio de Sousa, A.L. Simplício, H.C. de Sousa, C.M.M. Duarte, Preparation of glyceryl monostearate-based particles by PGSS-Application to caffeine, Journal of Supercritical Fluids 43 (2007) 120–125.
[13] M. Rodrigues, N. Peirico, H. Matos, E. Gomes De Azevedo, M.R. Lobato, A.J. Almeida, Microcomposites theophylline/hydrogenated palm oil from a PGSS process for controlled drug delivery systems, Journal of Supercritical Fluids 29 (2004) 175–184.
[14] J. Kerč, Z. Knez, S. Srčič, P. Senčar-Božič, Micronization of drugs using supercritical carbon dioxide, International Journal of Pharmaceutics 182 (1999) 33–39.
[15] E. Reverchon, G. la Porta, Terbutaline microparticles suitable for aerosol delivery produced by supercritical assisted atomization, International Journal of Pharmaceutics 258 (2003) 1–9.
[16] M. Sauceau, E. Rodier, J. Fages, Preparation of inclusion complex of piroxicam with cyclodextrin by using supercritical carbon dioxide, Journal of Supercritical Fluids 47 (2008) 326–332.
[17] I. Ribeiro Dos Santos, J. Richard, B. Pech, C. Thies, J.P. Benoit, Microencapsulation of protein particles within lipids using a novel supercritical fluid process, International Journal of Pharmaceutics 242 (2002) 69–78.
[18] R. Langer, Polymer-controlled drug delivery systems, Accounts of Chemical Research 26 (1993) 537–542.
[19] V.V. Khutoryanskiy, Hydrogen-bonded interpolymer complexes as materials for pharmaceutical applications, International Journal of Pharmaceutics 334 (2007) 15–26.
[20] M.M. Feldstein, T.L. Lebedeva, G.A. Shandryuk, S.V. Kotomin, S.A. Kuptsov, V.E. Igonin, T.E. Grokhovskaya, V.G. Kulichikhin, Complex formation in poly(vinyl pyrrolidone)–poly(ethylene glycol) blends, Polymer Science: Series A 41 (1999) 854–866.
[21] M.M. Feldstein, V.N. Tohmakhchi, L.B. Malkhazov, A.E. Vasiliev, N.A. Platé, Hydrophilic polymeric matrices for enhanced transdermal drug delivery, International Journal of Pharmaceutics 131 (1996) 229–242.
[22] I. Pasquali, L. Comi, F. Pucciarelli, R. Bettini, Swelling, melting point reduction and solubility of PEG 1500 in supercritical CO_2, International Journal of Pharmaceutics 356 (2008) 76–81.
[23] D Gourgouillon, M. Nunes Da Ponte, High pressure phase equilibria for poly(ethylene glycol)s + CO_2: experimental results and modelling, Physical Chemistry Chemical Physics 1 (1999) 5369–5375.
[24] J. Hao, M.J. Whitaker, G. Serhatkulu, K.M. Shakesheff, S.M. Howdle, Supercritical fluid assisted melting of poly(ethylene glycol): a new solvent-free route to microparticles, Journal of Materials Chemistry 15 (2005) 1148–1153.
[25] S.P. Nalawade, F. Picchioni, L.P.B.M. Janssen, Batch production of micron size particles from poly(ethylene glycol) using supercritical CO_2 as a processing solvent, Chemical Engineering Science 62 (2007) 1712–1720.
[26] T. Guadagno, S.G. Kazarian, High-pressure CO_2-expanded solvents: Simultaneous measurement of CO_2 sorption and swelling of liquid polymers with in-situ near-IR spectroscopy, Journal of Physical Chemistry B 108 (2004) 13995–13999.
[27] E. Weidner, V. Wiesmet, Ž. Knez, M. Kerget, M. Škerget, Phase equilibrium (solid–liquid–gas) in polyethyleneglycol-carbon dioxide systems, Journal of Supercritical Fluids 10 (1997) 139–147.
[28] K. Gong, R. Viboonkiat, I.U. Rehman, G. Buckton, J.A. Darr, Formation and characterization of porous indomethacin-PVP coprecipitates prepared using solvent-free supercritical fluid processing, Journal of Pharmaceutical Sciences 94 (2005) 2583–2590.
[29] S. Sethia, E. Squillante, Solid dispersion of carbamazepine in PVP K30 by conventional solvent evaporation and supercritical methods, International Journal of Pharmaceutics 272 (2004) 1–10.
[30] J. Von Schnitzler, R. Eggers, Mass transfer in polymers in a supercritical CO_2-atmosphere, Journal of Supercritical Fluids 16 (1999) 81–92.
[31] O.S. Fleming, K.L.A. Chan, S.G. Kazarian, High-pressure CO_2-enhanced polymer interdiffusion and dissolution studied with in situ ATR-FTIR spectroscopic imaging, Polymer 47 (2006) 4649–4658.
[32] R.S. Vartapetian, E.V. Khozina, J. Kärger, D. Geschke, F. Rittig, M.M. Feldstein, A.E. Chalykh, Self diffusion in poly(N-vinyl pyrrolidone)–poly(ethylene glycol) systems, Colloid and Polymer Science 279 (2001) 532–538.
[33] R.S. Vartapetian, E.V. Khozina, J. Kärger, D. Geschke, F. Rittig, M.M. Feldstein, A.E. Chalykh, Molecular dynamics in poly(N-vinylpyrrolidone)–poly(ethylene glycol) blends investigated by the pulsed-field gradient NMR method: effects of aging, hydration and PEG chain length, Macromolecular Chemistry and Physics 202 (2001) 2648–2656.
[34] J.M. Huang, S.J. Yang, Studying the miscibility and thermal behavior of polybenzoxazine/poly(ε-caprolactone) blends using DSC, DMA, and solid state 13C NMR spectroscopy, Polymer 46 (2005) 8068–8078.
[35] K. Backfolk, R. Holmes, P. Ihalainen, P. Sirviö, N. Triantafillopoulos, J. Peltonen, Determination of the glass transition temperature of latex films: comparison of various methods, Polymer Testing 26 (2007) 1031–1040.
[36] R. Hagen, L. Salmén, H. Lavebratt, B. Stenberg, Comparison of dynamic mechanical measurements and T_g determinations with two different instruments, Polymer Testing 13 (1994) 113–128.
[37] M.M. Feldstein, S.A. Kuptsov, G.A. Shandryuk, N.A. Platé, Relation of glass transition temperature to the hydrogen-bonding degree and energy in poly(N-vinyl pyrrolidone) blends with hydroxyl-containing plasticizers. Part 2. Effects of poly(ethylene glycol) chain length, Polymer 42 (2001) 981–990.
[38] X. Liu, Q. Wu, PP/clay nanocomposites prepared by grafting-melt intercalation, Polymer 42 (2001) 10013–10019.
[39] R.W. Gray, N.G. McCrum, Origin of the U relaxations in polyethylene and polyetrafluoroethylene, Journal of Polymer Science-Polymer Physics 7 (1969) 1329–1355.
[40] J.M. Yu, Y.S. Yu, P. Dubois, R. Jerome, Stereocomplexation of sPMMA-PBD-sPMMA triblock copolymers with isotactic PMMA. 1. Thermal and mechanical properties of stereocomplexes, Polymer 38 (1997) 2143–2154.
[41] M. Pouplin, A. Redl, N. Gontard, Glass transition of wheat gluten plasticized with water, glycerol, or sorbitol, Journal of Agricultural and Food Chemistry 47 (1999) 538–543.
[42] P.C. Painter, G.J. Pehlert, Y. Hu, M.M. Coleman, Infrared band broadening and interactions in polar systems, Macromolecules 32 (1999) 2055–2057.
[43] Y. Hu, H.R. Motzer, A.M. Etxeberria, M.J. Fernandez-Berridi, J.J. Iruin, P.C. Painter, M.M. Coleman, Concerning the self-association of N-vinyl pyrrolidone and its effect on the determination of equilibrium constants and the thermodynamics of mixing, Macromolecular Chemistry and Physics 201 (2000) 705–714.
[44] C.Y. Chiu, Y.J. Yen, S.W. Kuo, H.W. Chen, F.C. Chang, Complicated phase behavior and ionic conductivities of PVP-co-PMMA-based polymer electrolytes, Polymer 48 (2007) 1329–1342.
[45] P.E. Kireeva, G.A. Shandryuk, J.V. Kostina, G.N. Bondarenko, P. Singh, G.W. Cleary, M.M. Feldstein, Competitive hydrogen bonding mechanisms underlying phase behavior of triple poly(N-vinyl pyrrolidone)–poly(ethylene glycol)–poly(methacrylic acid-co-ethylacrylate) blends, Journal of Applied Polymer Science 105 (2007) 3017–3036.
[46] A. Martinez De Ilarduya, J.J. Iruin, M.J. Fernandez-Berridi, Hydrogen bonding in blends of phenoxy resin and poly(vinylpyrrolidone), Macromolecules 28 (1995) 3707–3712.
[47] C. Lau, Y. Mi, A study of blending and complexation of poly(acrylic acid)/poly(vinyl pyrrolidone), Polymer 43 (2001) 823–829.
[48] R.G. Wissinger, M.E. Paulaitis, Swelling and sorption in polymer–CO_2 mixtures at elevated pressures, Journal of Polymer Science, Part B: Polymer Physics 25 (1987) 2497–2510.
[49] Y.T. Shieh, J.H. Su, G. Manivannan, P.H.C. Lee, S.P. Sawan, W.D. Spall, Interaction of supercritical carbon dioxide with polymers. II. Amorphous polymers, Journal of Applied Polymer Science 59 (1996) 707–717.
[50] O. Muth, T. Hirth, H. Vogel, Polymer modification by supercritical impregnation, Journal of Supercritical Fluids 17 (2000) 65–72.

[51] R.S. Vartapetyan, E.V. Khozina, A.E. Chalykh, V.D. Skirda, M.M. Feldstein, J. rger, D. Geschke, Molecular mobility in a poly(ethylene glycol)–poly(vinyl pyrrolidone) blends: study by the pulsed gradient NMR techniques, Colloid Journal of the Russian Academy of Sciences: Kolloidnyi Zhurnal 65 (2003) 684–690.

[52] M.M. Feldstein, A. Roos, C. Chevallier, C. Creton, E.E. Dormidontova, Relation of glass transition temperature to the hydrogen bonding degree and energy in poly(N-vinyl pyrrolidone) blends with hydroxyl-containing plasticizers. 3. Analysis of two glass transition temperatures featured for PVP solutions in liquid poly(ethylene glycol), Polymer 44 (2003) 1819–1834.